KIĘC-KONONOWICZ, K., ZEJC, A. & KOLASA, K. (1989). *Abstracts of a Polish Pharmaceutical Society Meeting at Wroclaw*, Vol. 8, p. 60.
LAIDIG, K. E. (1989). *SADDLE* and *SADD2R. Part of the PROAIM PROperties of Atoms in Molecules Package*. McMasters Univ., Ontario, Canada.
MOTHERWELL, W. D. S. & CLEGG, W. (1978). *PLUTO78. Program for Plotting Molecular and Crystal Structures*. Univ. of Cambridge, England.
NALEWAJSKI, R. F. & KORCHOWIEC, J. (1989). *J. Mol. Catal.* **54**, 324-342.
NARDELLI, M. (1983). *Comput. Chem.* **7**, 95-98.
PFLUGRATH, J. & MESSERSCHMITT, A. (1991). *MADNES*. Small molecule version. Enraf-Nonius, Delft, The Netherlands.
RUEDENBERG, K. & SCHWARZ, W. H. E. (1990). *J. Chem. Phys.* **92**, 4956-4969.
SCROCCO, E. & TOMASI, J. (1978). *Adv. Quantum Chem.* **11**, 116-190.
SHELDRICK, G. M. (1980). *SHELX80. Program for Crystal Structure Determination*. Univs. of Cambridge, England, and Göttingen, Germany.
SHELDRICK, G.M. (1986). *SHELXS86. Program for Crystal Structure Solution*. Univ. of Göttingen, Germany.
SHI, Z. & BOYD, R. J. (1991). *J. Phys. Chem.* **95**, 4698-4701.
STEVENS, W. J., BASCH, H. & KRAUSS, M. (1984). *J. Chem. Phys.* **81**, 6026-6033.
STONE, A. J. (1981). *Chem. Phys. Lett.* **83**, 233-239.
WONG, M. G., DEFINA, J. A. & ANDREWS, P. R. (1986). *J. Med. Chem.* **29**, 562-572.
ZEJC, A., KIEĆ-KONONOWICZ, K., CHLON, G., KLEINROK, Z., KOLASA, K., PIETRASIEWICZ, T. & CZECHOWSKA, G. (1989). *Pol. J. Pharmacol. Pharm.* **41**, 483-493.

Acta Cryst. (1994). B**50**, 96–106

Solids Modelled by Crystal Field *Ab Initio* Methods. 5.* The Phase Transitions in Biphenyl from a Molecular Point of View

BY A. T. H. LENSTRA, C. VAN ALSENOY, K. VERHULST AND H. J. GEISE

University of Antwerp (UIA), Department of Chemistry, Universiteitsplein 1, *B*-2610 *Wilrijk, Belgium*

(*Received* 21 *January* 1992; *accepted* 26 *July* 1993)

Abstract

Using *ab initio* calculations at the 4-21G level and procedures for extrapolation to r_g geometry as well as using the electrostatic crystal field (ECF-MO) approach, the geometry and torsion potential were calculated for 1,1′-biphenyl in the gas phase, in the $P2_1/a$ lattice with $Z = 2$ and in the Pa lattice with $Z = 4$. At all stages excellent agreement is obtained with available diffraction data, including L_{22} librational components between 293 and 40 K. The following molecular picture emerged when the molecule goes from the gas phase through the solid-state phases biphenyl I, biphenyl II and biphenyl III. In the gas phase biphenyl is twisted ($|\varphi| = 45.7°$) with a relatively high torsion barrier [$\Delta E(\varphi) = 7.9$ kJ mol^{-1}], decreasing to $|\varphi| = 27°$ and $\Delta E(\varphi) = 3.0$ kJ mol^{-1} in the $P2_1/a$ lattice of biphenyl I. In $P2_1/a$, each molecule is librating (in dynamical disorder) between an image form ($\varphi = +27°$) and a mirror-image form ($\varphi = -27°$). At 40 K a phase transition to biphenyl II takes place in which half of the molecules freeze into the image and half into the mirror-image enantiomer. They form racemic pairs along the *ab* diagonals of the *Pa* lattice. Since $Z = 4$ in the *Pa* lattice, there are two types of racemic pairs, *viz.* *AA′* and *BB′* with $|\varphi(A)| = 37.7$ and $|\varphi(B)| = 38.9°$. The observed incommensurability along **a*b*** between 17 and 40 K (biphenyl II) is associated with order/disorder competition of *AA′* and *BB′* pairs. The observed incommensurability along **b*** below 17 K (biphenyl III) is associated with the slow disappearance of domain boundaries. These are stacking faults as a result of glide planes left as relics of the original $P2_1/a$ structure. The calculations attribute $\Delta H = 0.33$ kJ mol^{-1} to the transition at 40 K and $\Delta H = 0.17$ kJ mol^{-1} to the transitions through the various incommensurate phases including that at 17 K. The values compare very well with those obtained by calorimetry. The model also rationalizes observations such as the approximate doubling of the *b* axis at 40 K, the quasi-temperature independent long-range order of 0.67 and $|\langle\varphi\rangle| = 10°$ in biphenyl II, as well as the length of the incommensurate wavevector in biphenyl III.

Introduction

Biphenyl (Fig. 1) is known to exhibit a complex conformational behaviour which depends on the aggregation state and the temperature. The purpose of this work is to rationalize the energetical and geometrical phenomena which take place when the molecule goes from the gaseous state through the various solid-state phases, including those that are incommensurate. In his paper on the temperature-dependent torsion potential Busing (1983) has summarized the considerable body of existing literature on this matter, so that here we will mention only those investigations of immediate relevance.

* Part 4: Lenstra, Van Alsenoy, Popelier & Geise (1994).

Electron-diffraction studies in the gas phase have shown (Almenningen, Bastiansen, Fernholt, Cyvin, Cyvin & Samdal, 1985) that biphenyl is twisted with $|\varphi| = 44.4\ (1.2)^\circ$, where φ denotes the dihedral angle between the two planes of the phenyl rings. In the solid-state phase transitions have been observed at about 40 and 17 K. Several single-crystal X-ray and neutron diffraction analyses have been performed on the neutral and deuterated species, and it has been proved (Baudour, Toupet, Délugeard & Ghémid, 1986) that from room temperature down to 40 K the compound crystallizes in the centrosymmetric space group $P2_1/a$ with $Z = 2$. This implies that the molecule is planar at least on average. Standard diffraction procedures have difficulty in distinguishing between $\varphi = 0$ (ordering at molecular level), $\langle\varphi\rangle_{\text{position}} = 0$ (static disorder) and $\langle\varphi\rangle_{\text{time}} = 0^\circ$ (dynamic disorder). From measurements of the temperature dependence of librational parameters (Charbonneau & Délugeard, 1976; 1977) and phonon frequencies (Plakida, Belushkin, Natkaniec & Watsiutynski, 1983), the model $\langle\varphi\rangle_{\text{time}} = 0^\circ$ emerged as the best description of the high-temperature structure (HT structure) above 40 K. Between 40 and 17 K the HT b axis approximately doubles and the crystal shows incommensurate modulations in both the b^* and a^* directions (Cailleau, Moussa & Mons, 1979). At 17 K phase III appears in which the modulation in the a^* direction has vanished, that along b^* remains and the structure tends towards an ordering in space group Pa with $Z = 4$ but with φ modulated between $+10$ and -10° (Cailleau, Baudour & Zeyen, 1979; Baudour & Sanquer, 1983).

In order to pursue our research goal we use standard SCF-LCAO-MO procedures to calculate molecular models in the gas phase and we subsequently incorporate into these standard procedures a simple electrostatic crystal field (ECF-MO) to model the solid state. That is, the properties of a molecule in the solid state are taken to be those of a central molecule surrounded by electrical point charges. In the calculations the charge values are enumerated from *e.g.* a Mulliken population analysis and the charge positions are those of the crystallographic structure. Standard *ab initio* techniques are used to ensure self consistency (Almlöf & Wahlgren, 1973; Almlöf, Kvick & Thomas, 1973; Helgaker & Klewe, 1988). So far the procedure has successfully reproduced, both in direction and magnitude, the observed differences between the gaseous and solid-state geometries of cyanoformamide (Saebo, Klewe & Samdal, 1983), acetamide (Popelier, Lenstra, Van Alsenoy & Geise, 1989) and formamide (Popelier, Lenstra, Van Alsenoy & Geise, 1991). It was also successful in reproducing the librational and translational components of the temperature parameters in cubic acetylene, which helped to reveal deficiencies in standard crystallographic procedures and reconciled three puzzling experimental observations of the C≡C bond length (Popelier, Lenstra, Van Alsenoy & Geise, 1988; Popelier 1989). In these calculations the crystalline phase is regarded as an Einstein solid consisting of independent harmonic oscillators. Hence it was logical to avoid – at least in the initial steps – complex situations such as lattice relaxation, short-range order and incommensurate structures with their typical long-range order. Now, we wish to extend the scope towards incommensurate systems using the axial next nearest-neighbour Ising (ANNNI) model, starting from the results of Popelier (1989).

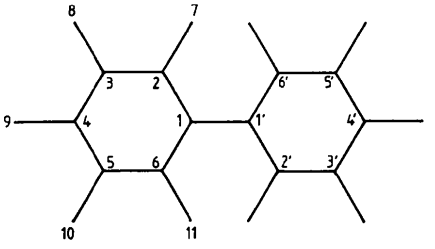

Fig. 1. Structural formula of biphenyl and atomic numbering scheme.

Biphenyl in the gas phase

The equilibrium geometry of an isolated biphenyl molecule, constrained to the observed symmetry D_2, was enumerated with the program *BRABO* (Van Alsenoy, 1988) using the 4-21G basis set (Pulay, Fogarasi, Pang & Boggs, 1979). This basis set was taken because of its favourable cost-to-benefit ratio. It has been shown (De Smedt, Vanhouteghem, Van Alsenoy, Geise & Schäfer, 1992) that with appropriate empirical corrections the results of the less demanding 4-21G calculations fit r_g bond lengths of state-of-the-art electron-diffraction experiments equally well as those of the intrinsically better 6-31G calculations. Such corrections not only eliminate the 4-21G artefacts but also introduce a vibrational correction, bridging the gap between the vibrationless *ab initio* model and the vibrating molecule actually observed. The calculations were considered converged when the largest residual force on any atom dropped below 10 pN. It is believed (Schäfer, 1983) that at this level of refinement bond lengths are within 0.0005 Å, valence angles within 0.2° and torsion angles within 0.5° of the 4-21G optimum value. Table 1 gives the comparison between the *ab initio* r_g geometry and the experimental geometry (Almenningen *et al.*, 1985). For a review of the multitude of previous *ab initio*, semi-empirical and molecular mechanics calculations we refer to

Häfelinger & Regelmann (1985, 1987). From their review and Table 1 it follows that, also in the case of biphenyl, the 4-21G and the 6-31G calculated r_g geometry are within one e.s.d. of the experimental values. Clearly the observed biphenyl structure represents the minimum energy conformer. Next, we enumerated the 4-21G energy of an isolated biphenyl molecule as a function of φ, while fixing the other internal parameters at their equilibrium value. This resulted in the symmetric, double-well torsion potential illustrated in Fig. 2. The calculated energy barrier height at $\varphi = 0°$ is 7.9 kJ mol^{-1}, in perfect agreement with the experimental value of 7.9 (1.8) kJ mol^{-1} in the gas phase (Almenningen *et al.*, 1985).

Table 1. *Experimental and calculated geometries of biphenyl in gas phase*

Distances in Å, angles in decimal degrees, e.s.d.'s in parentheses. See Fig. 1 for atomic numbering.

	Calculated 4-21G			Experimental	
	$C_{12}H_{10}$ r(4-21G)	$C_{12}H_{10}$ r_g*	$C_{12}H_{10}$ r_g†	$C_{12}H_{10}$ r_a	$C_{12}D_{10}$ r_a
C(1)—C(1′)	1.493	1.506	1.505	1.503 (4)	1.490 (4)
C(1)—C(2)	1.391	1.404	1.406	1.403 (4)	1.404 (5)
C(2)—C(3)	1.383	1.396	1.397	1.395 (6)	1.396 (6)
C(3)—(4)	1.384	1.397	1.398	1.396 (8)	1.396 (8)
C—H(*D*)	1.072	1.106	1.107	1.102 (2)	1.095 (2)
C(2)—C(1)—C(6)	118.7	118.7	118.7	118.7 (4)	117.8 (4)
C(1)—C(2)—C(3)	120.6	120.6	120.6	120.6 (2)	121.1 (2)
$\|\varphi\|$	45.7	45.7	46.8	46.8 (1.0)	47.0 (1.0)

* Transformed using $r_g = r$(4-21G) + δ with δ(C—C) = 0.013 and δ(C—H) = 0.034 Å (Geise & Pyckhout, 1989). No corrections are applied to angles.

† Transformed using $r_g = r_a + U_a^2/r_a$, with r_a and U_a values taken from the static model of Almenningen *et al.* (1985).

Biphenyl in the high-temperature solid state

Between room temperature and 40 K biphenyl crystallizes in the monoclinic space group $P2_1/a$ with $Z = 2$, in which the midpoints of the C(1)—C(1′) bonds are situated at [0,0,0] and [$\frac{1}{2}$,$\frac{1}{2}$,0] and coincide with the crystallographic inversion centres. As a result the HT solid-state model of biphenyl can be characterized by having $\varphi = 0°$ and a layer structure in which the *ab* planes cut halfway through the molecules. It seems as if the molecular symmetry goes from D_2 in the gas phase to D_{2h} in the monoclinic solid. Looking at the torsion-energy profile for an isolated molecule this change in symmetry would be strongly energy demanding. Since the torsion potential in the solid state may well be different from that in the gas phase, we decided to approach the former using the ECF-MO method. The central biphenyl moiety, described by its LCAO wavefunction, is surrounded by a coordinating shell of 36 biphenyl neighbours (*i.e.* a spherical cluster of 7 Å radius) positioned as in the $P2_1/a$ lattice. D_{2h} symmetry is assigned to each molecule, and all neighbours are represented by a Mulliken charge per atomic site, calculated from the central biphenyl. For justifications of this choice of cluster size and the use of Mulliken charges we refer to Popelier *et al.* (1988, 1991). The electrostatic field so generated is superimposed as a perturbation on the wavefunction of the central molecule and produces a change in the geometry and Mulliken charges of the latter moiety. These changes are then transferred to all coordinating neighbours and the process is repeated until the largest force leading to a shift in atomic position is smaller than 10 pN. We take this as the converged r(4-21G) geometry for the solid state.

When one wants to calculate the torsion potential of biphenyl in its $P2_1/a$ lattice, one obviously must keep the symmetry of the perturbing field fixed to $P2_1/a$, *i.e.* one must work with a rigid coordination of D_{2h} biphenyl neighbours. Also it matters how one rotates one phenyl ring with respect to the other. If one rotates one ring and fixes the position of the other, one introduces a twist ($\varphi \neq 0°$) into the central molecule, but also a rotation of its system of inertia axes. That is, one also introduces a rigid-body rotation of the central molecule in the field of the reference cluster. Then, the calculated energy changes contain a torsion as well as a rotation contribution. To avoid this by conserving the orientation of the inertia axes one has to rotate both rings over the same angle (φ/2), but in opposite directions. This procedure resulted in the calculated torsion potential in its $P2_1/a$ cluster given in Fig. 2. It

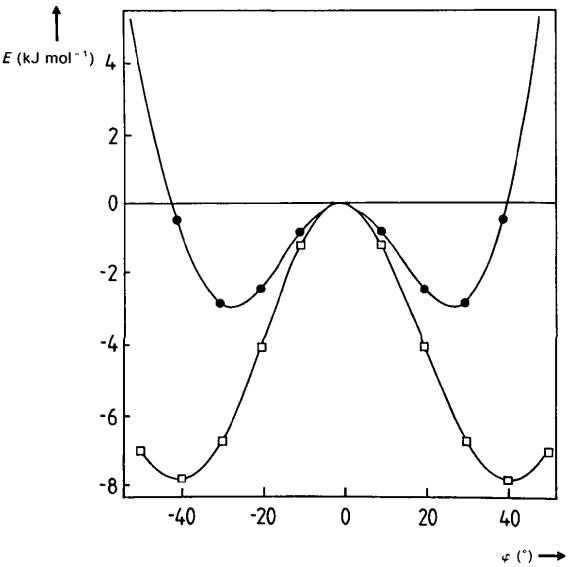

Fig. 2. The energy (kJ mol^{-1}) of an isolated biphenyl molecule (□) and of a biphenyl molecule in its $P2_1/a$ lattice (●) as a function of the torsion angle φ (decimal degrees).

is again a double-well potential, but the barrier height at $\varphi = 0°$ is reduced to 3 kJ mol^{-1} and the energy minima now occur at $\varphi = \pm 27°$. An experimental analysis of the biphenyl torsion in the $P2_1/a$ lattice has been given by Plakida *et al.* (1983). From the temperature dependence of phonon frequencies the authors arrived also at a symmetric double-well potential with a barrier height at $\varphi = 0°$ of 3.4 kJ mol^{-1} and energy minima at $\varphi = \pm 20°$.

Encouraged by the agreement with experiment, we venture to explore further the molecular model behind the calculations. Whereas the gas-phase model of biphenyl clearly is an equilibrium structure, the planar solid-state model is not because it corresponds to a local maximum in the torsion energy. In view of the low barrier height the HT structure can be interpreted as a time-averaged structure ($\langle\varphi\rangle_{\text{time}} = 0°$). The increase in symmetry from D_2 in the gas phase to D_{2h} in the $P2_1/a$ solid has nothing to do with the actual molecular equilibrium geometry. The solid-state calculations reveal that neighbouring molecules have a flattening effect upon the central biphenyl molecule (*cf.* $|\varphi| = 46°$ in the gas phase and $|\varphi| = 27°$ in the $P2_1/a$ solid).

Simultaneously, the torsion barrier is reduced at $\varphi = 0°$ such that biphenyl in the HT phase can alternate its geometry from 'image' (φ taken *e.g.* positive) to 'mirror image' (φ taken negative). This dynamic disorder produces at the molecular site a racemic mixture as the best fitting static model.

Interactions between a biphenyl molecule with neighbouring molecules are not restricted to the solid phase. Similar interactions are present in the liquid and in solution. Hence, the model above qualitatively rationalizes the conformational behaviour of biphenyl in all phases and tallies with experimental evidence. UV measurements have led to $|\varphi| \simeq 18°$ in the melt (Tinland, 1968) and to $|\varphi| = 22\,(4)°$ in *n*-heptane solution (Suzuki, 1959). Vibrational spectra (Eaton & Steele, 1973) have produced $|\varphi| = 32\,(2)°$ in solution. Temperature-dependent ^{1}H NMR analyses (Kurland & Wise, 1964) of 4,4′-dideuterobiphenyl in methylcyclohexane, chloroform–carbon tetrachloride mixture and in carbon disulfide have led to estimates of the torsion barrier between 2 and 4 kJ mol^{-1}. Our model unifies the view on the behaviour of biphenyl and *p*-terphenyl. Biphenyl's conformation is governed by a double-well potential with a barrier height of 3 kJ mol^{-1}, which is to be compared with the experimental results of Baudour, Cailleau & Yelon (1977), demonstrating that the libration of the central phenyl ring in *p*-terphenyl is governed by a double-well potential with a barrier height of 2.5 kJ mol^{-1}. We believe that this suffices to show that a real difference in behaviour between *p*-terphenyl and biphenyl is very unlikely, in contrast to the opinion of Baudour *et al.* (1986).

Influence of temperature on the libration of biphenyl in the $P2_1/a$ lattice

Diffraction studies revealed in the $P2_1/a$ structure of biphenyl an unusually large libration component L_{22}, linked to rotations around the long molecular axis. For example, at 110 K a value of $L_{22} = 46$ deg^2 is observed to be compared with values of about 3 deg^2 for L_{11} and L_{33} (Charbonneau & Délugeard, 1976). Table 2 gives root-mean-square values for L_{22} as a function of the temperature, as summarized by Baudour *et al.* (1986). The r.m.s. values follow a standard pattern, *i.e.* they become smaller at lower temperatures. Some have used this trend to assign a single-well potential to the biphenyl C(1)—C(1′) libration. Such a conclusion, however, rests on a circular argumentation. Translation (T) and libration (L) components are evaluated from observed U values, which themselves are only adequate parameters to describe atomic motions governed by harmonic restoring forces (*i.e.* a single-well potential). In view of our anharmonic torsion-energy profile the experimentally derived U values may have a precise numerical value but they lack a firm physical meaning. Thus, if our anharmonic torsion-energy profile is correct, then it is incorrect to interpret the experimental U values as harmonic parameters. Below we will show how the anharmonic potential can be used to reproduce the pseudo-harmonic behaviour of L_{22}.

The anharmonic torsion potential provides the intramolecular contribution to L_{22}. Using the Boltzmann expression $n(\varphi) = \exp(-\delta E/kT)$, this potential is easily translated into a series of temperature-dependent population-density functions, $P(\varphi|T)$. Since $E(\varphi)$ is symmetric around $\varphi = 0$, we always find the average torsion $\langle\varphi\rangle = 0$ [*i.e.* the first moment of $P(\varphi|T)$]. For the r.m.s. values $\langle\varphi^2\rangle^{1/2}$ [*i.e.* the second moment of $P(\varphi|T)$], we find values of 13.2°, virtually independent of temperature (see Table 2, $\langle\varphi^2\rangle^{1/2}$ column). Thus, the calculated intramolecular torsion contributions to L_{22} are already larger than the total, so-called observed L_{22} values. However, if one wants to compare the model r.m.s. values with the experimentally derived data one obviously must use the same parameter definitions. If one wants, as we do, to bring the model data to the experimental basis, one must approach the anharmonic torsion potential (Fig. 2) by a harmonic one. In other words, we must fit a parabolic function centred at $\varphi = 0°$ to the potential of Fig. 2(*b*), which is equivalent to fitting a Gaussian function centred at $\varphi = 0°$ to the population density $P(\varphi|T)$. In doing so we have forced our anharmonic model into a pseudo-harmonic description with a harmonic potential generating a normal distributed population density. The second moment of the latter population density

is the pseudo-harmonic contribution of the molecular torsion to L_{22} (Table 2, column 'pseudo-harmonic'). Now the model results follow the same trend as the experimental ones, but the former are systematically too small because the intermolecular contribution to L_{22} has not been included yet. The missing contribution is the L_{22} component linked to the rigid-body rotation of biphenyl in the $P2_1/a$ lattice. While preserving in all molecules the D_{2h} symmetry connected to the $P2_1/a$ lattice, we rotated the central molecule over 10 and 20° along the C(1)—C(1′) axis within the field of its 36 neighbours and found the cluster energy to increase by 11.7 and 17.0 kJ mol^{-1}, respectively. If we now assume for simplicity that the rigid-body rotation between −10 and +10° is governed by a harmonic potential $E = fL^2$, then the force constant f is 117 J mol^{-1} deg^2. Since $L^2 = RT/2f$, it is easy to calculate the rigid-body contribution to L_{22} as a function of temperature. The results are given in Table 2, 'rigid body' column. When we sum the mean-square values listed in Table 2 as 'pseudo-harmonic' and 'rigid body', we obtain the expected values for the L_{22} libration. In spite of all approximations, the agreement with the experimental values is convincing: the crystal-field approximation (ECF-MO) reproduces the observed structural information well within experimental error. This underlines the reliability of the model for temperatures above T_c (40 K), which separates the HT from the LT phase. In our opinion the calculated crystal potential proved sufficiently reliable to drop the verifications of agreement between calculated and experimental geometry of biphenyl in the $P2_1/a$ lattice. Instead we give a detailed argumentation of that decision, because it illustrates some general problems in X-ray crystallography.

Before a meaningful comparison between calculated and experimental geometrical parameters can be made, they must be transformed to the same geometrical basis, *e.g.* r_α° geometry, defined upon averaged nuclear coordinates in the vibrational ground state (*cf.* Popelier *et al.*, 1988, and references cited therein). The ECF-MO geometry may be brought to the r_α° basis using $r_\alpha^\circ = r(\text{ECF-MO}) + K + \delta$, where K is the contribution of the vibration perpendicular to the bond under consideration and δ the empirical correction mentioned earlier (in *Biphenyl in the gas phase*). On the experimental side, the required internuclear distances may result from neutron diffraction analyses and high-order X-ray refinements, to which corrections for thermal translational and rotational effects have been applied. Unfortunately, however, as outlined above, standard X-ray procedures for these corrections assume harmonic vibrations and thus produce in the case of biphenyl strongly biased geometries. One way to cope with the problem is to start from positional coordinates and temperature parameters derived from the ECF-MO population densities [such as $P(\varphi|T)$] and calculate a suitable set of (hkl) intensities. When this intensity set is subjected to the same series of crystallographic computations as the experimental set, then the two sets of refined parameters can be compared. In the case of acetylene (Popelier, 1989), we have shown that such an approach reproduces the experimental trends in geometry. For biphenyl we did not want to repeat this type of checking again. Since the standard experimental geometry obtained is biased towards a 'wrong' (*i.e.* pseudo-harmonic) model without immediately apparent consequences, the extra information gained in the comparison is small compared with the effort invested. Moreover, *via* the Boltzmann equation there is a one-to-one relation between the ECF-MO potential functions and the associated population density functions. The first moment of these density functions yields the geometric parameters and the second moment the thermal parameters. The latter are more appropriate to the biphenyl case and thus we considered it most appropriate to establish the reliability of the ECF-MO energy functions by checking the thermal parameters.

Table 2. *Root-mean-square libration* (°) *along the central* C(1)—C(1′) *bond at various temperatures*

Temp. (K)	$(L_{22})^{1/2}$	$\langle\varphi^2\rangle^{1/2}$	Pseudo-harmonic	Rigid body	Pseudo harmonic + rigid body
293	10.5 (1.4)	13.1	7.9	10.5	13.1
110	6.8 (1.0)	13.2	6.0	3.9	7.1
40	5.0 (1.0)	13.2	3.9	1.4	4.1

The molecular trigger behind the phase transition at 40 K

Above the critical temperature T_c (40 K), the planarity of the biphenyl structure in its $P2_1/a$ lattice is the result of dynamic disorder. The calculated torsion potential for the solid state suggests a critical temperature of about 120 K (*cf.* barrier height is equal to $3RT_c$). The real T_c will be lower because the crystal-field model does not take lattice-relaxation effects into account.

Below T_c the time-averaged structure ceases to be planar. Each biphenyl molecule changes from a 'racemic average' into one of the two enantiomeric alternatives, with an expected torsion angle φ of +27 or −27° (see Fig. 2), and the midpoints of C(1)—C(1′) cease to be molecular inversion centres. This is in line with the Raman spectroscopic evidence of Bree & Edelson (1978) who reported $T_c = 42$ K for $C_{12}H_{10}$ and $T_c = 38$ K for $C_{12}D_{10}$ and described the phase transition as a gradual one. Since a C—D bond is about 0.01 Å shorter than a C—H bond (see Table 1), the torsion barrier at $\varphi = 0°$ will be slightly

lower for the deuterated compound because of a decrease in steric hindrance. Thus, the proposed molecular model behind the phase transition agrees with the observed T_c sequence. Also, the gradual nature of the phase transition is easily understood as an order/disorder phenomenon linked to the image/mirror image competition in the LT structure.

We will now analyse the phase transition as quantitatively as possible, exploiting the possibilities of the ECF-MO approach. Let us assume that below T_c the molecular inversion symmetry is lost, but that the overall packing of the molecules in the lattice does not change. Then, the LT phase of biphenyl will have the same unit cell as the HT phase, but the space group becomes either $P2_1$ or *Pa*. In one cluster constructed using *Pa* building rules, and in another using $P2_1$ rules, we optimized the geometry of biphenyl to the respective solid-state equilibrium geometries. In both cases the geometry converged to nearly identical biphenyl entities. Starting from a 'mirror image' ($\varphi = -27°$) biphenyl as the asymmetric building block and central moiety, the largest difference occurred in the torsions, which converged to $\varphi = -30.2°$ in *Pa* and to $\varphi = -26.9°$ in $P2_1$. The molecular energy of biphenyl in the *Pa* cluster was 3.5 kJ mol^{-1} lower than in the $P2_1$ cluster. Subsequently, we calculated in both clusters the energy profile connected to the torsion. The results are depicted in Fig. 3, in which the energy of the *Pa* potential at $\varphi = -30.2°$ is arbitrarily set at $E = 0$, and the $P2_1$ potential is moved upwards over 3.5 kJ mol^{-1} to make $E = 0$ at $\varphi = -26.9°$. Again, we find double-well potentials, but the symmetry around $\varphi = 0°$ is lost, even to the extent that replacement of the original 'mirror image' biphenyl molecule by an 'image' biphenyl lowers the energy. To interpret this finding one should be aware that a (*e.g.*) *Pa* lattice is quasi-infinite, but a *Pa* cluster is finite, although *Pa* building rules are used in the construction. Hence, if we extend the clusters to real lattices, both proposed packing schemes are self-destructive, because conservation of crystal (lattice) symmetry is incompatible with minimum-energy rules. It appears that the loss of a molecular inversion centre is not the only change in the structure that takes place at T_c. We need to identify another structural change which allows the LT structure to conserve its molecular packing scheme.

The change in the packing at 40 K

The transition of the average biphenyl geometry from D_{2h} (HT phase) to D_2 (LT phase) eliminates the inversion centres at [0,0,0] and [$\frac{1}{2}$,$\frac{1}{2}$,0]. In the previous section we tacitly assumed that the other inversion centres of the HT phase are lost as well. This might be an oversimplification, which we will now consider.

In the HT phase the biphenyl layers are separated by the *c* axis. The subsequent layers are connected by a lattice translation and an inversion through [0,0,$\frac{1}{2}$]. When only the translation is preserved at the phase transition the non-planar biphenyl molecule generates along the *c* axis, say 'image'–'image' sequences. When, however, the inversion through [0,0,$\frac{1}{2}$] is preserved, 'image'–'mirror image' sequences are generated and the phase transition should be attended by a doubling of the *c* axis. Fixing the torsion φ at 27° (minimum of $P2_1$ potential, Fig. 3), *i.e.* selecting an 'image'–'image' sequence along the *c* axis, leads to a series of intermolecular short contacts between neighbouring molecules which are geometrically acceptable. For the alternative ($\varphi = +30$, $\varphi = -30°$, minima of *Pa* potential, Fig. 3) 'image'–'mirror image' sequence, however, a number of short contacts becomes too small to be compatible with standard van der Waals distances. Thus, from a geometrical point of view [0,0,$\frac{1}{2}$] ceases to be an inversion centre when biphenyl changes from D_{2h} to D_2.

At this point we will set a first step to overcome the weakness of describing the solid state as a collection of independent oscillators (Einstein model) by introducing explicitly short-range interactions between neighbouring molecules. We treated two D_2 biphenyl molecules, situated at [0,0,0] and [0,0,1] as in the $P2_1/a$ lattice (*i.e.* equivalent atoms separated by 9.51 Å, the length of the *c* axis), as a supermolecule combining them into one single wavefunction. The energy of the 'image'–'image' dimer was found to be 21 kJ mol^{-1} lower than the energy of the

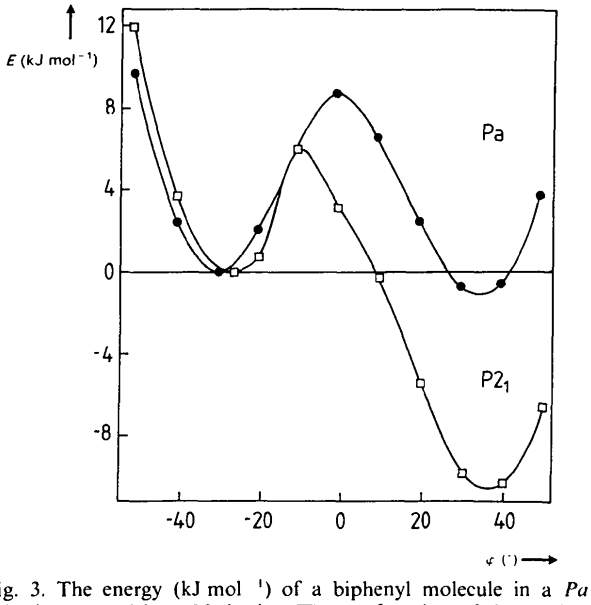

Fig. 3. The energy (kJ mol^{-1}) of a biphenyl molecule in a *Pa* lattice (●) and in a $P2_1$ lattice (□) as a function of the torsion angle φ (decimal degrees).

'image'–'mirror image' dimer. This larger energy difference strongly suggests that at 40 K each layer along the *c* axis will be a perfect copy of a reference layer in the (0,0,1) plane. Hence, the second element that changes at the phase transition has to be found within this layer. Let us now re-examine the results of the previous section in a two-dimensional perspective. Fig. 4 depicts the local cluster geometry in the *ab* plane for each of the four minima on the $E(\varphi)$ potential (see Fig. 3). Introducing the Ising nomenclature, the HT phase with $\langle\varphi\rangle_{\text{time}} = 0°$ may be called a paramagnetic phase. The four structures of Fig. 4 may be designated as ferromagnetic (4*a*), disturbed ferromagnetic (4*b*), antiferromagnetic (4*c*) and disturbed antiferromagnetic (4*d*). These structure models were identified in the previous section as unsatisfactory, suggesting that an Ising model using only nearest-neighbour interactions is inadequate. The energy estimates (Figs. 3 and 4) corroborate this, because it is impossible to contract the values into a single interaction energy. They can, however, be summarized by two interaction energies, *viz.* a nearest-neighbour interaction energy V_1 along [1,1,0] and [1,$\bar{1}$,0], and a second-nearest-neighbour interaction energy V_2 along [0,1,0]. These interactions happen to be identical to the interaction scheme proposed by Heine & Price (1985). The crystal-field relative energies fit to $V_1 = 1$ kJ mol^{-1}, by which an ↑↓ combination along [1,1,0] is favoured over an ↑↑ sequence, and to $V_2 = 3$ kJ mol^{-1}, by which an ↑↓ sequence along [0,1,0] is preferred over an ↑↑ sequence. The results allow the conclusion that the local packing scheme (Fig. 4) influences *inter alia* the energy of the central oscillator. Indeed, it is the feedback between the oscillator and its coordination which enables one to identify the near-neighbour interaction energies V_1 and V_2 and the preference of an image/mirror image setting of the molecules in the LT solid over a structure containing one single enantiomer. Having overcome the first barrier of the Einsteinian concept by showing that two interaction energies are sufficient to reproduce the four *ab initio* cluster energies, it seemed logical to continue the analysis along the lines of the axial next nearest-neighbour Ising (ANNNI) model. For an excellent review of the subject we refer to Selke (1988). The phase diagram typical for the ANNNI model is shown in Fig. 5. In biphenyl the ratio $V_2/V_1 \simeq 3$ is well above the critical value of $+\frac{1}{2}$, *i.e.* we expect at 0 K biphenyl to have ideally a (2,2)-antiphase structure. It is also evident that the paramagnetic HT phase and the LT (2,2)-antiphase are separated by modulated 'in-between' structures.

In the HT phase the molecules along the **ab** diagonals are related by the glide plane and the twofold screw axis. For biphenyl moieties with D_2 symmetry the energy component V_1 favours an ↑↓ combination and is thus only in line with the glide plane. Along the *b* axis V_2 expresses preference for an ↑↓ sequence and is thus compatible with the inversion centre at [0,$\frac{1}{2}$,0] present in the HT structure, but neither in $P2_1$ nor *Pa*. Therefore, a doubling of the *b* axis at T_c seems to be required. The above analysis in combination with the cluster energies strongly suggests for the 0 K phase a preference for the *Pa* periodic lattice.

Starting from the (1,1)-antiphase model of biphenyl in its HT unit cell and replacing the ↑↓ sequence along the **ab** diagonals by an ↑↑↓↓ sequence we obtain a model for the LT (2,2)-antiphase structure. This process, shown in Fig. 6, introduces a doubling of the *b* axis and the concomitant loss of half of the glide planes. Cailleau, Baudour & Zeyen (1979) indeed observed the *Pa* space group and doubling of the *b* axis in the first crystallographic analysis of biphenyl below T_c. At that time the authors used an order/disorder model to interpret the structure. Later Baudour & Sanquer (1983) replaced the order/disorder description by a model

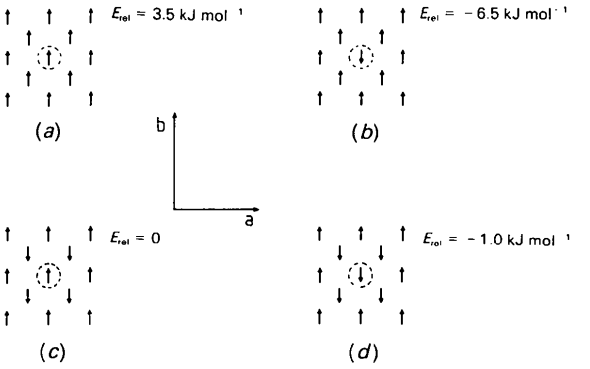

Fig. 4. Representation of local cluster geometry in the *ab* plane and relative energies (kJ mol^{-1}). An 'image' biphenyl molecule is shown as ↓, a 'mirror-image' one as ↑. The four minima of Fig. 3 give: A biphenyl cluster with $P2_1$ symmetry built on an ↑ asymmetric unit in which (*a*) the central molecule (encircled) is also an ↑ molecule, (*b*) the central molecule is replaced by an ↓ molecule. Also shown is the biphenyl cluster with *Pa* symmetry built on an ↑ asymmetric unit in which (*c*) the central moiety is also an ↑ molecule, (*d*) the central molecule is replaced by an ↓ molecule.

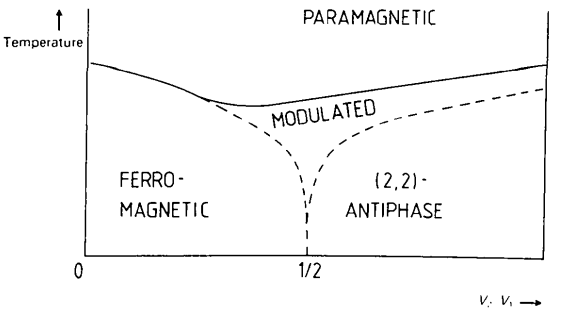

Fig. 5. Phase diagram of the three-dimensional ANNNI model in a lattice with an interaction scheme as in biphenyl.

based on structure modulations. Both descriptions are in line with the (2,2)-antiphase model and ANNNI expectations.

The proposed changes in the lattice connected with the phase transition are also logical from another point of view. Charbonneau & Delugeard (1977) noted in the diffraction pattern of biphenyl at room temperature a diffuse spot at $(\frac{1}{2},\frac{1}{2},0)$. In our opinion the spot indicates that at 300 K biphenyl already has a certain non-zero short-range order along [1,1,0]. At T_c the associated long-range order has deviated sufficiently from zero to trigger an order/disorder phase transition.

Other consequences of the (2,2)-antiphase description will be confronted with experimental results in the next section.

Experimental evidence for the ANNNI model

At 23 K the long-range order in biphenyl was found to be 0.67 and the averaged torsion $|\langle\varphi\rangle| = 10°$ (Cailleau, Baudour & Zeyen, 1979). These values follow quantitatively from the model. We recall that at the phase transition the change from D_{2h} to D_2 symmetry can be described such that each biphenyl 'racemic mixture' freezes into one of the two enantiomeric forms. That is each biphenyl molecule has equal chance to become ↓ to which the model assigns $\varphi = +30°$, or to become ↑ to which $\varphi = -30°$ is assigned. The process produces a random chain of biphenyl enantiomers with D_2 symmetry. In other words, the competition between the survival of the HT lattice periodicity along the b axis (producing an ↑↑ pair or an ↓↓ pair depending upon the choice of origin) and the survival of the inversion centre at $[0,\frac{1}{2},0]$ (producing an ↑↓ pair) ends in a draw. Hence, the most likely distribution of enantiomers along **b** is then two of one kind and one of the other (↑↑↓ or ↓↓↑), that is a (3,3)-antiphase. With two molecules per cell this directly translates into an order parameter $\frac{2}{3}$ and $|\langle\varphi\rangle| = 10°$. The model also calls for a significant correlation between the long-range order and the torsion parameter. Unfortunately, Cailleau, Baudour & Zeyen (1979) do not discuss this aspect of their refinement.

Let us now focus the attention on energy. According to Cullick & Gerkin (1977), the enthalpy change ΔH connected to the phase transition at 40 K is approximately 0.29 kJ mol^{-1}. From Fig. 6 it is clear that a structural change from the (1,1)-antiphase to the (2,2)-antiphase forces half of the biphenyl molecules to change their enantiomeric form. From Figs. 3 and 4 we derive that such a transition in space group Pa (see Fig. 6*a*) produces an energy gain of 1 kJ mol^{-1}, and hence the transition (1,1)-antiphase →(2,2)-antiphase would reduce the energy by 0.5 kJ mol^{-1}. Given a random biphenyl ordering along **b** and thus a long-range order of $\frac{2}{3}$, the model estimates the effective energy gain $\Delta E =$ 0.33 kJ mol^{-1}.

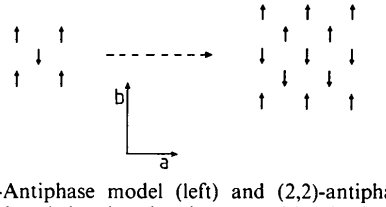

Fig. 6. (1,1)-Antiphase model (left) and (2,2)-antiphase model (right) of biphenyl showing the phase transition in the *ab* plane.

To conclude this section we briefly discuss the incommensurate nature of the biphenyl lattice between the HT phase and the 0 K structure. Here we follow the logic of Heine & Price (1985), *i.e.* a one-dimensional phonon approximation along the b axis. For the energy one has:

$$I_t\omega^2(q) = V_0 + 4V_1\cos(1/2qb) + 2V_2\cos(qb)$$

where I_t is the torsional moment of inertia. By differentiating this expression we find the minimum frequency of $\omega(q)$ to occur when $\cos(1/2qb) = -V_1/2V_2$. Substitution of V_1 and V_2 leads to the length of the incommensurate wavevector $\mathbf{q} = 0.55\,\mathbf{b}^*$. This value matches satisfactorily with the satellite positions in biphenyl III observed by Cailleau, Moussa & Mons (1979). It is gratifying to note that an incommensurate period of ~20 unit cells along the b axis can be inferred from the *ab initio* cluster energies, although the clusters have a diameter of only three times the b axis. The clusters used are commensurate (ferro- and antiferromagnetic) and incommensurate (the perturbed analogue). The cluster calculations give the interaction energies V_1 and V_2 which dictate the phonon energy in the above mentioned Fourier series. It is this series that is instrumental in extrapolating the *ab initio* cluster calculations beyond their direct cluster size.

So far, the agreement between experiment and the ECF-MO described (2,2)-antiphase model is excellent and warrants more detailed exploration.

The solid-state optimization of the (2,2)-antiphase structure

In the (2,2)-antiphase lattice (Fig. 6, right) we optimized the solid-state geometry of the two crystallographically independent biphenyl moieties located at [0,0,0] and $[0,\frac{1}{2},0]$ in the LT unit cell. We started from biphenyl molecules with torsion angles $\varphi = +35$ and $\varphi = -30°$, in line with the results in the *Pa* (1,1)-antiphase structure (Fig. 3). The radius of the coordinating cluster of molecules around the two central entities was increased from 7 to 12 Å to ensure that possible effects linked to the doubled b

axis were included in the electrostatic field perturbation. As a consequence the number of molecules in the coordinating cluster increased from 36 to 66. Both central molecules converged (largest residual force on any atom less than 10 pN) to optimized geometries in which equivalent bond distances and valence angles differ by no more than 0.003 Å and 0.7°, respectively. The torsion angle of one biphenyl (henceforth called *A*) converged to $\varphi(A) = +37.7°$, and of the other (henceforth called *B*) to $\varphi(B) = -38.9°$, with molecules *A* being 9.3 kJ mol^{-1} less stable than molecules *B*.

Starting from the converged equilibrium geometries we again enumerated the torsion potentials for *A*- and *B*-type molecules. The two profiles are shown in Fig. 7, in which the energy of the *B*-type potential at $\varphi = -38.9°$ is arbitrarily set at $E = 0$ and the *A*-type potential is moved upwards over 9.3 kJ mol^{-1} to make $E(A) = 0$ at $\varphi(A) = 37.7°$. One notes from Fig. 7 that replacement of an original *A* molecule by its enantiomeric alternative (henceforth called *A'*) costs about 16 kJ mol^{-1}. The same holds for replacement of *B*-type molecules by *B'* alternatives. Thus, the proposed (2,2)-antiphase model reconciles the conservation of lattice symmetry with the principle of minimum energy. This is a significant improvement compared with the (1,1)-antiphase model.

We can now interpret on the molecular level what takes place in biphenyl when the temperature decreases from 40 to 0 K. In the biphenyl I structure, above $T_c = 40$ K the lattice behaves as a collection of individual molecules. It may be visualized in dynamic disorder with molecules librating between $\varphi = +28$ and $\varphi = -28°$. Below T_c the minimum energy is attained by molecules having $\varphi = 38°$. Thus, during the phase transition individual molecules are allowed to adjust their geometry towards the gas-phase structure ($\varphi = 46°$), *i.e.* towards the minimum energy of the unperturbed molecule. The adjustment is made possible by dimer formation. Along [1,1,0] the (2,2)-antiphase model resulted in two different dimers, *viz.* *AA'* and *BB'* dimers, where *A* molecules are related to *A'* molecules, and *B* to *B'*, by a glide plane along the *a* direction. In each dimer the sum of the torsion angles is exactly 0°. Averaged planarity, above T_c regarded as a property of the individual molecule, is maintained below T_c as a dimer property. But even at room temperature, a sufficient amount of these dimers persist to cause the diffuse reflection $(\frac{1}{2},\frac{1}{2},0)$ in the room-temperature diffraction pattern ($P2_1/a$).

The set of structures between 40 and 17 K, collectively known as biphenyl II, is characterized by modulations along the diagonals [1,1,0] and [1,−1,0] in the *ab* plane. It is easy to see that disorder of the *AA'* and *BB'* dimers – differing in their geometry only by 1.2° in $|\varphi|$ – is responsible for the incommensurability along the diagonals. Below 17 K the *AA'*/*BB'* disorder disappears giving rise to the biphenyl III set of structures in which the incommensurability is associated with the quasi-phonon model with a calculated modulation of 0.55**b***. The model points to stacking faults as the origin of the latter modulation. The most likely stacking error is a glide plane which should be absent in the ideal (2,2)-antiphase, but which survived as a relic of the original $P2_1/a$ symmetry. As illustrated in Fig. 8, this stacking fault does not affect the dimer condition $\varphi(A) + \varphi(A') = \varphi(B) + \varphi(B') = 0$. The glide-plane error, however, acts as a domain boundary linking phase and antiphase domains and most importantly changing the sequence along the *b* axis from *AB* into *BA* (and *A'B'* into *B'A'*). This explains the observed

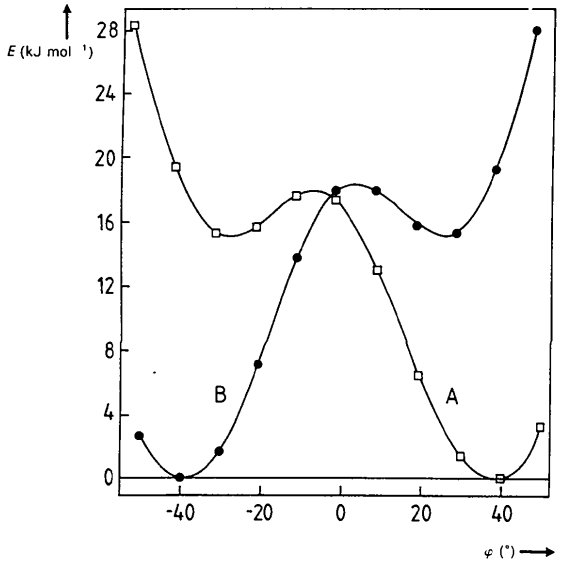

Fig. 7. The energy (kJ mol^{-1}) of an *A*-type biphenyl molecule (□) and of a *B* type (●) as a function of the torsion angle φ. See text for further explanation.

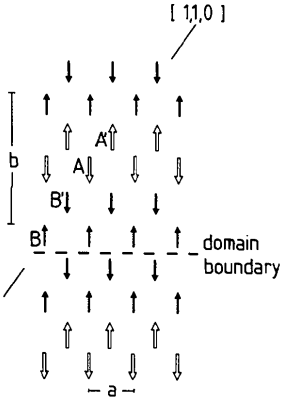

Fig. 8. The final *Pa* lattice with the (2,2)-antiphase along [1,1,0] and occasional extra glide plane stacking faults acting as domain boundaries.

[0,1,0] modulation. In our opinion further reduction of the temperature will ultimately lead to a collapse of the domain boundaries and to the ideal (2,2)-antiphase *Pa* structure. The latter structure is commensurate ($q = 0.5\mathbf{b}^*$) and represents in our opinion the ground state of the biphenyl lattice at 0 K. This view is in keeping with Benkert's (1987) description of biphenyl III as a metastable phase.

Benkert, Heine & Simons (1987) summarize the available evidence of biphenyl as follows: (i) a phase lock-in when T is reduced to 4 K has not been observed and (ii) the perturbation in biphenyl III is not a sinusoidal, but a squared wave. The squared-wave pattern perfectly matches our model: the modulation along **b** is caused by phase/antiphase domain boundaries, in which phase and antiphase are connected to a biphenyl torsional shift from $\varphi = -38$ to $\varphi = +38°$. In the (2,2)-antiphase, the ideal sequence along the b axis (see Fig. 8) is *ABABAB*. Because of the presence of a domain wall (designated by |), this sequence is modified into *AB|BABA*. A phason-induced shift of the domain boundary leads to a new local sequence given by *ABA|ABA*. The latter two molecular sequences have virtually identical energies. As a consequence a phase lock-in is very unlikely.

At this point our modelling exercise has to end, because it is only guided by energy considerations. Phason-related shifts in the phase/antiphase boundary give each molecule the choice between $\varphi = -38$ and $\varphi = +38°$, which automatically leads to an entropy component of k ln 2 per molecule. This entropy contribution helps to stabilize the incommensurate biphenyl III structure at the expense of the (2,2)-antiphase ground state, which has no entropy contribution per molecule (k ln 1 = 0).

The molecular mechanism behind the phase transitions explains the hitherto puzzling behaviour of the long-range order parameter. It was found to be constant at 0.67 between 40 and 23 K and possibly beyond. Normally one expects that an increase in lattice ordering becomes visible with an increase of the long-range order parameter. In the model, the order parameter is zero in biphenyl I and changes to 0.67 at 40 K. The value 0.67 is associated with a random order of 'image' and 'mirror-image' molecules (irrespective of actual φ values) along the b axis (see previous section). This particular disorder persists even below 17 K and other temperature-induced increases in ordering have no effect.

Finally, we would like to discuss some thermodynamical aspects. Evidently, above 40 K the biphenyl molecules assume an energetically unfavourable packing ($P2_1/a$), which is counterbalanced by entropy (disorder). We calculated that a total of 0.5 kJ mol^{-1} can be gained for the Gibbs free energy by trading in all entropy contributions for reductions of the enthalpy. We recall that the model predicts a gain of 0.33 kJ mol^{-1} (experimentally observed 0.29 kJ mol^{-1}) for the step biphenyl I → biphenyl II at 40 K. Atake & Chihara (1980) observed anomalies in the heat capacity of biphenyl in the temperature regions between 30 and 47 K, and between 7.5 and 14 K. The concomitant enthalpy changes are 0.19 and 0.003 kJ mol^{-1}, respectively. The ECF-MO model associates the first ΔH with the disappearance of the AA'/BB' disorder and the second ΔH with the reduction of the number of domain boundaries. The experimental value 0.19 + 0.003 kJ mol^{-1} is again gratifyingly close to the theoretical 0.50 − 0.33 = 0.17 kJ mol^{-1}, which has not yet been accounted for. The gradual disappearance of the various disorders agrees naturally with the observed broadness of the anomalies.

Dr P. Popelier is thanked for his help in the many calculations. KV gratefully acknowledges financial support as a predoctoral fellow by the Belgian organization IWONL. CVA thanks the Belgian National Science Foundation (NFWO) for an appointment as onderzoeksleider. This text represents research results of the Belgian Program on Interuniversity Attraction Poles initiated by the Belgian State, Prime Minister's Office, Science Policy Programming. The scientific responsibility, however, remains with the authors.

References

ALMENNINGEN, A., BASTIANSEN, O., FERNHOLT, L., CYVIN, B. N., CYVIN, S. J. & SAMDAL, S. (1985). *J. Mol. Struct.* **128**, 59–76.
ALMLÖF, J., KVICK, Å. & THOMAS, J. O. (1973). *J. Chem. Phys.* **59**, 3901–3906.
ALMLÖF, J. & WAHLGREN, U. (1973). *Theor. Chim. Acta*, **28**, 161–168.
ATAKE, T. & CHIHARA, H. (1980). *Solid State Commun.* **35**, 131–134.
BAUDOUR, J. L., CAILLEAU, H. & YELON, W. B. (1977). *Acta Cryst.* B**33**, 1773–1780.
BAUDOUR, J. L. & SANQUER, M. (1983). *Acta Cryst.* B**39**, 75–84.
BAUDOUR, J. L., TOUPET, L., DÉLUGEARD, Y. & GHÉMID, S. (1986). *Acta Cryst.* C**42**, 1211–1217.
BENKERT, C. (1987). *J. Phys. C*, **20**, 3369–3379.
BENKERT, C., HEINE, V. & SIMONS, E. H. (1987). *J. Phys. C*, **20**, 3337–3354.
BREE, A. & EDELSON, M. (1978). *Chem. Phys. Lett.* **55**, 319–322.
BUSING, W. (1983). *Acta Cryst.* A**39**, 340–347.
CAILLEAU, H., BAUDOUR, J. L. & ZEYEN, C. M. E. (1979). *Acta Cryst.* B**35**, 426–432.
CAILLEAU, H., MOUSSA, F. & MONS, J. (1979). *Solid State Commun.* **31**, 521–524.
CHARBONNEAU, G.-P. & DÉLUGEARD, Y. (1976). *Acta Cryst.* B**32**, 1420–1423.
CHARBONNEAU, G.-P. & DÉLUGEARD, Y. (1977). *Acta Cryst.* B**33**, 1586–1588.
CULLICK, A. S. & GERKIN, R. E. (1977). *Chem. Phys.* **23**, 217–230.
DE SMEDT, J., VANHOUTEGHEM, F., VAN ALSENOY, C., GEISE, H. J. & SCHÄFER, L. (1992). *J. Mol. Struct.* **259**, 289–305.
EATON, V. J. & STEELE, D. (1973). *J. Chem. Soc. Faraday Trans.* **2**, 1601–1608.

GEISE, H. J. & PYCKHOUT, W. (1989). In *Stereochemical Applications of Gas Phase Electron Diffraction*, Part 1, ch.10, edited by I. HARGITTAI & M. HARGITTAI. New York: VCH Publishers.
HÄFELINGER, G. & REGELMANN, C. (1985). *J. Comput. Chem.* **6**, 368–376.
HÄFELINGER, G. & REGELMANN, C. (1987). *J. Comput. Chem.* **8**, 1057–1065.
HEINE, V. & PRICE, S. L. (1985). *J. Phys. C*, **18**, 5259–5278.
HELGAKER, T. U. & KLEWE, B. (1988). *Acta Chem. Scand. Ser. A*, **42**, 269–272.
KURLAND, R. J. & WISE, W. B. (1964). *J. Am. Chem. Soc.* **86**, 1877–1879.
LENSTRA, A. T. H., VAN ALSENOY, C., POPELIER, P. & GEISE, H. J. (1994). To be published.
PLAKIDA, N. M., BELUSHKIN, A. V., NATKANIEC, I. & WASIUTYNSKI, T. (1983). *Phys. Status Solidi B*, **118**, 129–133.
POPELIER, P. (1989). PhD thesis, Univ. of Antwerpen, Belgium.
POPELIER, P., LENSTRA, A. T. H., VAN ALSENOY, C. & GEISE, H. J. (1988). *Acta Chim. Scand. Ser. A*, **42**, 539–543.
POPELIER, P., LENSTRA, A. T. H., VAN ALSENOY, C. & GEISE, H. J. (1989). *J. Am. Chem. Soc.* **111**, 5658–5660.
POPELIER, P., LENSTRA, A. T. H., VAN ALSENOY, C. & GEISE, H. J. (1991). *Struct. Chem.* **2**, 3–9.
PULAY, P., FOGARASI, G., PANG, F. & BOGGS, J. E. J. (1979). *J. Am. Chem. Soc.* **101**, 2550–2560.
SAEBO, S., KLEWE, B. & SAMDAL, S. (1983). *Chem. Phys. Lett.* **97**, 499–502.
SCHÄFER, L. (1983). *J. Mol. Struct.* **100**, 51–73.
SELKE, W. (1988). *Phys. Rep.* **170**, 213–264.
SUZUKI, H. (1959). *Bull. Chem. Soc. Jpn*, **32**, 1340–1361.
TINLAND, B. (1968). *Acta Phys. Acad. Sci. Hung.* **25**, 111–114.
VAN ALSENOY, C. (1988). *J. Comput. Chem.* **9**, 620–626.

Acta Cryst. (1994). B**50**, 106–112

Structures and Photochemical Reactions of 1-(9-Anthryl)-2-aroylethylenes: Competing *cis–trans* Isomerization and Skeletal Rearrangement

BY YUKIE MORI AND KOKO MAEDA*

Department of Chemistry, Faculty of Science, Ochanomizu University, Otsuka, Bunkyo-ku, Tokyo 112, *Japan*

(*Received* 27 *May* 1993; *accepted* 23 *August* 1993)

Abstract

(*Z*)-3-(9-Anthryl)-1-phenylpropenone, *cis*-(I), $C_{23}H_{16}O$, $M_r = 308.38$, orthorhombic, $P2_12_12_1$, $a = 14.992\ (3)$, $b = 19.124\ (4)$, $c = 5.614\ (1)$ Å, $V = 1609.4\ (6)$ Å^3, $Z = 4$, $D_x = 1.273$ g cm^{-3}, $\mu = 0.071$ mm^{-1}, $F(000) = 648$, $R = 0.061$ for 1101 observed reflections; (*Z*)-2-(9-anthrylmethylene)-1-indanone, *cis*-(III), $C_{24}H_{16}O$, $M_r = 320.40$, monoclinic, $P2_1/a$, $a = 11.641\ (5)$, $b = 13.914\ (10)$, $c = 10.399\ (6)$ Å, $\beta = 102.71\ (4)^\circ$, $V = 1643.1\ (16)$ Å^3, $Z = 4$, $D_x = 1.295$ g cm^{-3}, $\mu = 0.072$ mm^{-1}, $F(000) = 672$, $R = 0.060$ for 2321 observed reflections; (*Z*)-2-(9-anthrylmethylene)-1-tetralone, *cis*-(IV), $C_{25}H_{18}O$, $M_r = 334.39$, monoclinic, $P2_1/c$, $a = 9.106\ (4)$, $b = 25.977\ (9)$, $c = 7.478\ (2)$ Å, $\beta = 96.76\ (5)^\circ$, $V = 1756.6\ (11)$ Å^3, $Z = 4$, $D_x = 1.264$ g cm^{-3}, $\mu = 0.070$ mm^{-1}, $F(000) = 704$, $R = 0.070$ for 1594 observed reflections; (*E*)-2-(9-anthrylmethylene)-1-tetralone, *trans*-(IV), $C_{25}H_{18}O$, $M_r = 334.39$, monoclinic, $P2_1/c$, $a = 12.032\ (2)$, $b = 13.608\ (3)$, $c = 10.829\ (3)$ Å, $\beta = 95.78\ (2)^\circ$, $V = 1764.1\ (7)$ Å^3, $Z = 4$, $D_x = 1.259$ g cm^{-3}, $\mu = 0.070$ mm^{-1}, $F(000) = 704$, $R = 0.055$ for 1985 observed reflections. *cis*-(I), *cis*-(III) and *cis*-(IV) exist in a conformation similar to each other, in which the anthracene plane forms a large dihedral angle [75.5 (3), 64.5 (1) and 67.2 (2)°, respectively] with the ethylene plane. These compounds rapidly undergo photochemical *cis–trans* isomerization in solution, while irradiation of *cis*-(I) in the solid state almost exclusively afforded an intramolecular [4 + 2] cyclization product, suggesting that the isomerization would be inhibited by crystal-lattice constraints. *cis*-(IV) also underwent [4 + 2] cyclization in the solid state, while in the case of *cis*-(III) only *cis–trans* isomerization was observed both in solution and in the solid state. A comparison of the molecular structures of *cis*-(I), -(III) and -(IV) suggested that the C(6)···O distance, where a new bond would be formed in the cyclization process, should be related to the photochemical reactivity.

* To whom correspondence should be addressed.

Introduction

It was reported that 3-(9-anthryl)-1-phenylpropenone (I) underwent photochemical skeletal rearrangement into a furano-annelated 5*H*-dibenzo[*a*,*d*]cycloheptene (II) through [4 + 2] cycloaddition involving the conjugated dienone moiety in a benzene solution (Becker, Becker, Sandros & Andersson, 1985). This photochemical transformation is quite inefficient in solution due to competition with energy-wasting *cis–trans* isomerization. In general, crystalline-state reactions tend to be controlled by packing arrangements of the reacting molecules and therefore selectivity among competing reaction pathways will differ from that observed in solution. In the case of (I) it is